Accurate Solution of the Volume Integral Equation for High-Permittivity Scatterers

Jörg P. Kottmann and Olivier J. F. Martin

***Abstract*—We present a formalism based on the method of moment to solve the volume integral equation using tetrahedral (3-D) and triangular (2-D) elements. We introduce a regularization scheme to handle the strong singularity of the Green's tensor. This regularization scheme is extended to neighboring elements, which dramatically improves the accuracy and the convergence of the technique. Scattering by high-permittivity scatterers, like semiconductors, can be accurately computed. Furthermore, plasmon–polariton resonances in dispersive materials can also be reproduced.**

***Index Terms*—Electromagnetic (EM) scattering, finite-element methods, Green's function, moment methods, plasmons, regularization, resonance, singular value decomposition.**

I. Introduction

ELECTROMAGNETIC (EM) scattering by high-permittivity materials is a very important issue since most semiconductors have a large index at optical wavelengths. Typical values are, for example, $\varepsilon = 11.20$ for gallium arsenide at 1 [μm] or $\varepsilon = 16.65 + 0.23i$ for silicon at 546 [nm] [1]. Unfortunately, the computation of scattering by such a system is difficult because of the very short effective wavelength inside the material and the strong field discontinuities at its boundary. Furthermore, practical situations often involve a combination of localized scatterers with semiinfinite backgrounds, like silicon particles on a wafer, defects buried in a multilayered semiconductor, etc. Such intricate boundary conditions can be difficult to handle for many computational techniques.

Our approach is based on the volume integral equation (VIE)

$$\mathbf{E}(\mathbf{r}) = \mathbf{E}^0(\mathbf{r}) + \int_{\mathrm{V}} \mathrm{d}\mathbf{r}' \mathbf{G}(\mathbf{r}, \mathbf{r}') \cdot V(\mathbf{r}') \mathbf{E}(\mathbf{r}') \qquad (1)$$

to compute the total scattered field $\mathbf{E}(\mathbf{r})$, when a system described by a dielectric function $\varepsilon(\mathbf{r})$ embedded in an infinite homogeneous background medium ε_0 is illuminated with an incident field $\mathbf{E}^0(\mathbf{r})$ (throughout the paper, we assume nonmagnetic materials and an $\exp(-i\omega t)$ time dependence for the fields). In (1), $V(\mathbf{r})$ represents the scatterer polarizability

$$V(\mathbf{r}) = k_0^2(\varepsilon(\mathbf{r}) - \varepsilon_0) \qquad (2)$$

with k_0 the vacuum wavenumber and $\mathbf{G}(\mathbf{r}, \mathbf{r}')$ the Green's tensor.

Manuscript received June 21, 1999; revised January 26, 2000. This work was supported by the Swiss National Science Foundation.

The authors are with the Electromagnetic Fields and Microwave Electronics Laboratory, Swiss Federal Institute of Technology, ETH-Zentrum, ETZ, CH-8092 Zurich, Switzerland (e-mail: kottmann@ifh.ee.ethz.ch).

Publisher Item Identifier S 0018-926X(00)07714-0.

The major advantage of this approach lies in the fact that only the scatterer must be discretized. Moreover, nontrivial backgrounds like multilayer structures can be included in the Green's tensor [2].

Different techniques can be used to solve (1) numerically. In the coupled-dipole approximation [3], [4] the scatterer is discretized with cubes and the field assumed constant over each element. Although there have been several efforts to overcome its intrinsic limitations [5]–[7], this method does not seem suitable for high permittivities [8].

Another approach to solve (1) is to use finite elements. Since the work of Richmond [9], the finite-element method has been broadly used in computational EMs [10]–[14]. Here, the geometry can be well discretized by elements like tetrahedra, and the variation of the field over an element can be modeled using nontrivial basis functions.

However, applying the method of finite elements to the VIE is difficult because of the strong singularity of the Green's tensor [15], [16]. To handle this singularity, a modified point-matching method [17] and modified Galerkin methods were proposed [18], [19]. Moreover, the strong singularity of the Green's tensor can be circumvented by moving the derivatives that lead to the singularity of the Green's tensor onto the test and basis functions using partial integration. To avoid surface integrals, rooftop functions defined on cubical or tetrahedral elements can then be used [10], [20]–[24]. In the same context, Mendes and Arvas computed high-permittivity two-dimensional (2-D) scatterers, using a special set of basis functions that avoids both spurious volume and surface charges [25]. However, this type of basis functions cannot be extended to three-dimensional (3-D) problems.

A formalism independent on the type of basis functions requires a regularization scheme to remove the singularity of the Green's tensor [26]–[29]. In this paper, we introduce such a scheme. In Section II, a general formalism is proposed for the solution of the VIE using tetrahedral elements. We show how to remove the singularity of the Green's tensor by subtracting a term that can be integrated analytically. To improve accuracy, this regularization scheme is extended to neighboring elements. In Section III, we apply this general formalism to 2-D geometries. Numerical results to assess the accuracy of the formalism are presented in Section IV.

II. Formalism

A. Basic Equations

The Green's tensor $\mathbf{G}(\mathbf{r}, \mathbf{r}')$ in (1) can be written as [4]

$$\mathbf{G}(\mathbf{r}, \mathbf{r}') = \left(\mathbf{1} + \frac{\nabla\nabla}{k_0^2}\right) g(\mathbf{r}, \mathbf{r}') \qquad (3)$$

with $g(\mathbf{r}, \mathbf{r}')$ the scalar Green's function:

$$g(\mathbf{r}, \mathbf{r}') = \frac{\exp ik_0 R}{4\pi R}, \quad \text{for 3-D}$$
$$g(\mathbf{r}, \mathbf{r}') = \frac{i}{4} \mathrm{H}_0^{(1)}(k_\rho \rho) \exp(ik_z Z), \quad \text{for 2-D} \tag{4}$$

where we introduced $R = |\mathbf{R}| = |\mathbf{r} - \mathbf{r}'|$. For 2-D, the geometry has a translation symmetry in z-direction and we introduced the transverse coordinate ρ defined by $\mathbf{R} = (\rho, Z)$ and the transverse wave vector $\mathbf{k}_\rho$: $\mathbf{k} = (\mathbf{k}_\rho, k_z)$.

To solve (1) we use the method of moments and divide the scatterer into N tetrahedra (triangles in 2-D) with volumes $\mathcal{V}_A$ (surfaces $\mathcal{V}_A$ in 2-D), $A = 1, \ldots, N$. On each element, A we assume a constant polarizability V_A and define m scalar basis functions $f_A^1, \ldots, f_A^m$ that vanish outside A. For the field $\mathbf{E}(\mathbf{r})$ inside the scatterer, we write

$$\mathbf{E}(\mathbf{r}) = \sum_{A=1}^{N} \sum_{j=1}^{m} \mathbf{a}_A^j f_A^j \tag{5}$$

with $\mathbf{a}_A^j$ the unknown vectorial coefficients. Inserting (5) in (1), symmetrizing by multiplication with $V(\mathbf{r})$ and applying Galerkin's scheme, we obtain the system of $mN \times mN$ vectorial equations

$$\sum_{j=1}^{m} b_A^{ij} \mathbf{a}_A^j - \sum_{B=1}^{N} \sum_{j=1}^{m} \mathbf{d}_{AB}^{ij} \cdot \mathbf{a}_B^j = \mathbf{e}_A^i, \; \begin{matrix} i = 1, \ldots, m \\ A = 1, \ldots, N \end{matrix} \tag{6}$$

with

$$b_A^{ij} = V_A \int_{\mathcal{V}_A} \mathrm{d}\mathbf{r} f_A^i(\mathbf{r}) f_A^j(\mathbf{r}) \tag{7}$$

$$\mathbf{e}_A^i = V_A \int_{\mathcal{V}_A} \mathrm{d}\mathbf{r} f_A^i(\mathbf{r}) \mathbf{E}^0(\mathbf{r}) \tag{8}$$

$$\mathbf{d}_{AB}^{ij} = V_A V_B \int_{\mathcal{V}_A} \mathrm{d}\mathbf{r} f_A^i(\mathbf{r}) \int_{\mathcal{V}_B} \mathrm{d}\mathbf{r}' \mathbf{G}(\mathbf{r}, \mathbf{r}') f_B^j(\mathbf{r}'). \tag{9}$$

The numerical solution of (6) gives the unknown coefficients for the field inside the scatterer. The field outside the scatterer can then be determined from the field inside the scatterer using (1).

B. Evaluation of the Integrals

Standard Gaussian integration technique is applied to evaluate the integrals in (7)–(9). To carry out this numerical quadrature, we map each element A on the canonical element with the transformation T_A [Fig. 1(a)]. Since the Gaussian points and the basis functions are originally defined on the canonical element, we will need the inverse transformation T_A^{-1} [Fig. 1(b)]:

$$\mathbf{r}_A(\boldsymbol{\xi}) = \mathbf{R}_A^1 \left(1 - \sum_{i=1}^{\mathrm{D}} \xi_i\right) + \sum_{i=1}^{\mathrm{D}} \mathbf{R}_A^{i+1} \xi_i, \quad A = 1, \ldots, N. \tag{10}$$

In (10), D is the space dimension (3 or 2), $\mathbf{R}_A^1, \ldots, \mathbf{R}_A^{\mathrm{D}+1}$ are the edges of element A, and $\boldsymbol{\xi} = (\xi_1, \ldots, \xi_{\mathrm{D}})$ is our new, *local* coordinate [Fig. 1(a)].

On the canonical element, we define η Gaussian integration points $\boldsymbol{\xi}^1, \ldots, \boldsymbol{\xi}^\eta$ and their weights $w^1, \ldots, w^\eta$ [Fig. 1(b)]. The corresponding *global* Gaussian points $\mathbf{r}_A^1, \ldots, \mathbf{r}_A^\eta$ on element A are given by inserting $\boldsymbol{\xi}^1, \ldots, \boldsymbol{\xi}^\eta$ in the transformation (10) [Fig. 1(b)]. The m basis functions $\phi_1(\boldsymbol{\xi}), \ldots, \phi_m(\boldsymbol{\xi})$ are also first defined on the canonical element. They are related to the global basis functions $f_A^i(\mathbf{r})$ on element A via the transformation (10), i.e.

$$f_A^i[\mathbf{r}_A(\boldsymbol{\xi})] = \phi^i(\boldsymbol{\xi}). \tag{11}$$

Using (10) and (11), we perform the integration on tetrahedron A by Gaussian quadrature. Equations (7)–(9) become

$$b_A^{ij} = \mathrm{V}_A J_A \left(\sum_{\alpha=1}^{\eta} w^\alpha \phi^i(\boldsymbol{\xi}^\alpha) \phi^j(\boldsymbol{\xi}^\alpha) \right) \tag{12}$$

$$\mathbf{e}_A^i = \mathrm{V}_A J_A \left(\sum_{\alpha=1}^{\eta} w^\alpha \phi^i(\boldsymbol{\xi}^\alpha) \mathbf{E}^0(\mathbf{r}_A^\alpha) \right) \tag{13}$$

$$\mathbf{d}_{AB}^{ij} = \mathrm{V}_A J_A \mathrm{V}_B \cdot \left[\sum_{\alpha=1}^{\eta} w^\alpha \phi^i(\boldsymbol{\xi}^\alpha) \underbrace{\left(\int_{\mathcal{V}_B} \mathrm{d}\mathbf{r}' \mathbf{G}(\mathbf{r}_A^\alpha, \mathbf{r}') f_B^j(\mathbf{r}') \right)}_{\mathbf{I}_{AB}} \right] \tag{14}$$

with J_A the Jacobian of the transformation (10). It represents the volume of element A in units of the volume of the canonical element (1/6 in 3-D and 1/2 in 2-D).

With (12) and (13), we have numerical expressions for the coefficients b_A^{ij} and $\mathbf{e}_A^i$ of (6). Note that for polynomial basis functions $\phi^i(\boldsymbol{\xi})$ the coefficients b_A^{ij} can also be evaluated analytically [30]. To evaluate the tensorial coefficients $\mathbf{d}_{AB}^{ij}$ we must distinguish two cases depending whether the elements A and B are different or coincide.

1) Evaluation of $\mathbf{I}_{AB}$ for Different Elements: When $A \neq B$, we can apply standard Gaussian integration to $\mathbf{I}_{AB}$ in (14) and obtain

$$\mathbf{I}_{AB} = J_B \left(\sum_{\beta=1}^{\eta} \mathbf{G}\left(\mathbf{r}_A^\alpha, \mathbf{r}_B^\beta\right) w^\beta \phi^j(\boldsymbol{\xi}^\beta) \right). \tag{15}$$

Note that, even located in different elements, the two Gaussian points $\mathbf{r}_A^\alpha$ and $\mathbf{r}_B^\beta$ can be very close to each other, which leads to an inaccurate value for $\mathbf{I}_{AB}$ using (15) because of the singular behavior of the Green's tensor for small arguments. A workaround for this will be proposed in Section II-B-3.

2) Regularization of $\mathbf{I}_{AB}$ for Identical Elements: For $A = B$ we have to introduce a regularization scheme for the evaluation of $\mathbf{I}_{AA}$ because of the strong singularity of the Green's tensor for $\mathbf{r}' = \mathbf{r}_A^\alpha$ ($\sim 1/R^3$ in 3-D and $\sim 1/R^2$ in 2-D).

The main idea of the regularization is to subtract from the integrand a function with the same singular behavior, but which can be integrated analytically. This is fulfilled by

$$\mathbf{I}_{AA} = \mathbf{I}_{AA}^{\mathrm{R}} + \mathbf{I}_{AA}^{\mathrm{S}} \tag{16}$$

where we choose for the regular part

$$\mathbf{I}_{AA}^{\mathrm{R}} = \int_{\mathcal{V}_A} \mathrm{d}\mathbf{r}' \cdot \left[\mathbf{G}(\mathbf{r}_A^\alpha, \mathbf{r}') f_A^j(\mathbf{r}') - \left(\frac{\nabla\nabla}{k_0^2} g^{\mathrm{S}}(\mathbf{r}_A^\alpha, \mathbf{r}') \right) \phi^j(\boldsymbol{\xi}^\alpha) \right] \tag{17}$$

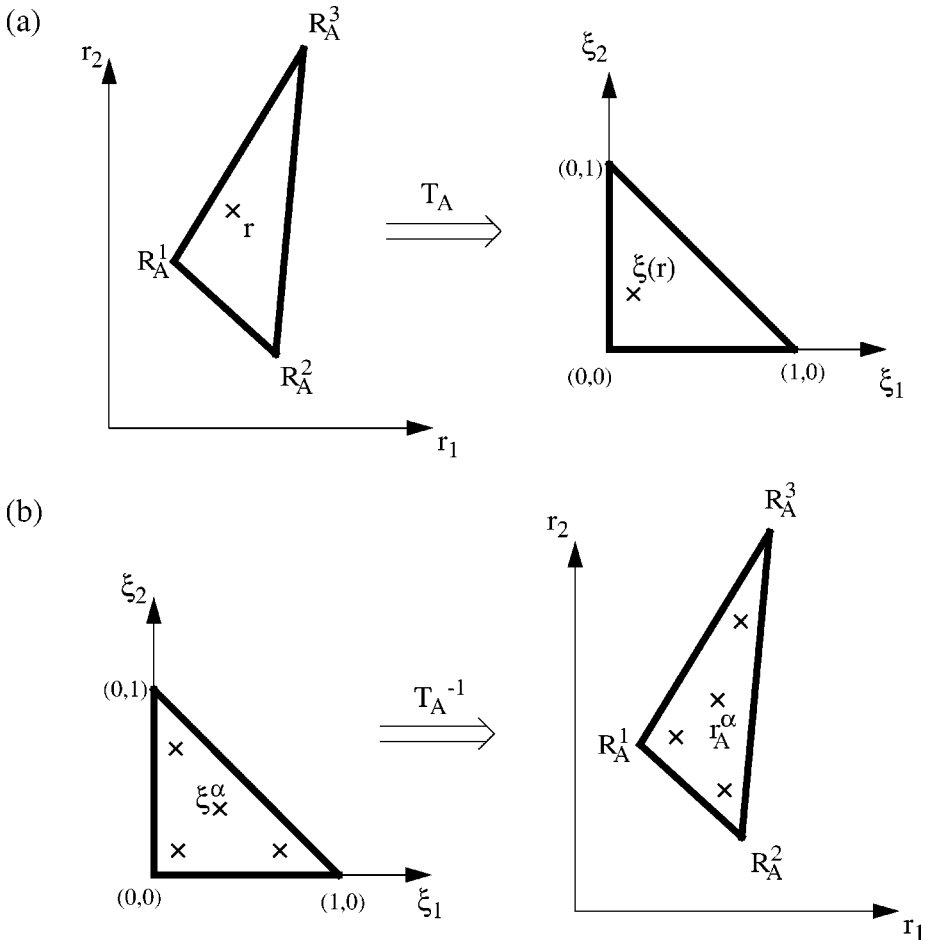

Fig. 1. Affine transformation. (a) Transformation T_A of triangle A onto the canonical element. (b) Inverse transformation T_A^{-1}. The Gaussian points and the basis functions are originally defined on the canonical element.

and for the singular part

$$\mathbf{I}_{AA}^{\mathrm{S}} = \phi^j(\boldsymbol{\xi}^\alpha) \int_{\mathcal{V}_A} \mathrm{d}\mathbf{r}' \frac{\nabla\nabla}{k_0^2}\, g^{\mathrm{S}}(\mathbf{r}_A^\alpha, \mathbf{r}') \tag{18}$$

with $g^{\mathrm{S}}(\mathbf{r}, \mathbf{r}')$ the static Green's function:

$$g^{\mathrm{S}}(\mathbf{r}, \mathbf{r}') = \frac{1}{4\pi R}, \qquad \text{for 3-D} \tag{19}$$

$$g^{\mathrm{S}}(\mathbf{r}, \mathbf{r}') = -\frac{1}{2\pi}\log(\rho), \quad \text{for 2-D.} \tag{20}$$

Note in (17) the important relation $f_A^j(\mathbf{r}_A^\alpha) = \phi^j(\boldsymbol{\xi}^\alpha)$. The operator $\nabla\nabla$ in (17), (18), and in the following has to be applied for $\mathbf{r} = \mathbf{r}_A^\alpha$.

The integrand in (17) is still singular for $\mathbf{r}' = \mathbf{r}_A^\alpha$. However, this singularity is now weak and Gaussian quadrature can be applied to the integral with a special treatment if the integration variable $\mathbf{r}'$ is near $\mathbf{r}_A^\alpha$ [Fig. 2(a)]. For the numerical value of $\mathbf{I}_{AA}^{\mathrm{R}}$ we take

$$\mathbf{I}_{AA}^{\mathrm{R}} = \sum_{\beta=1,\,\beta\neq\alpha}^{\eta} \Bigg\{ J_A w^\beta \Bigg[\mathbf{G}(\mathbf{r}_A^\alpha, \mathbf{r}_A^\beta)\phi^j(\boldsymbol{\xi}^\beta) - \left(\frac{\nabla\nabla}{k_0^2}\, g^{\mathrm{S}}(\mathbf{r}_A^\alpha, \mathbf{r}_A^\beta)\right)\phi^j(\boldsymbol{\xi}^\alpha) \Bigg] \Bigg\}$$
$$+ \int_{\mathcal{S}_A^\alpha} \mathrm{d}\mathbf{r}' \Bigg[\mathbf{G}(\mathbf{r}_A^\alpha, \mathbf{r}') f_A^j(\mathbf{r}') - \left(\frac{\nabla\nabla}{k_0^2}\, g^{\mathrm{S}}(\mathbf{r}_A^\alpha, \mathbf{r}')\right)\phi^j(\boldsymbol{\xi}^\alpha) \Bigg] \tag{21}$$

where $\mathcal{S}_A^\alpha$ is a sphere with volume $w^\alpha J_A$ centered at $\mathbf{r}_A^\alpha$ [Fig. 2(a)]. This approach is illustrated in Fig. 2(a).

In a further step, let us divide the integral in (21) into two terms:

$$\int_{\mathcal{S}_A^\alpha} \mathrm{d}\mathbf{r}' \left[\mathbf{G}(\mathbf{r}_A^\alpha, \mathbf{r}') f_A^j(\mathbf{r}') - \left(\frac{\nabla\nabla}{k_0^2}\, g^{\mathrm{S}}(\mathbf{r}_A^\alpha, \mathbf{r}')\right)\phi^j(\boldsymbol{\xi}^\alpha) \right]$$
$$= \phi^j(\boldsymbol{\xi}^\alpha) \int_{\mathcal{S}_A^\alpha} \mathrm{d}\mathbf{r}' \left(\mathbf{G}(\mathbf{r}_A^\alpha, \mathbf{r}') - \frac{\nabla\nabla}{k_0^2}\, g^{\mathrm{S}}(\mathbf{r}_A^\alpha, \mathbf{r}') \right)$$
$$+ \int_{\mathcal{S}_A^\alpha} \mathrm{d}\mathbf{r}' \mathbf{G}(\mathbf{r}_A^\alpha, \mathbf{r}') \left[f_A^j(\mathbf{r}') - f_A^j(\mathbf{r}_A^\alpha) \right] \tag{22}$$

where we used $\phi^j(\boldsymbol{\xi}^\alpha) = f_A^j(\mathbf{r}_A^\alpha)$. The first integral does not depend on the explicit form of the basis functions and can easily be performed analytically. The second integral, however, depends on the explicit form of the basis functions. It vanishes for constant basis functions since $f_A^j(\mathbf{r}') = f_A^j(\mathbf{r}_A^\alpha)$. For higher-order basis functions, the integrand must be expanded in a Laurent series with respect to $|\mathbf{r}' - \mathbf{r}_A^\alpha|$ using the spherical coordinates of $\mathbf{r}' - \mathbf{r}_A^\alpha$, and retaining only the singular and constant terms with

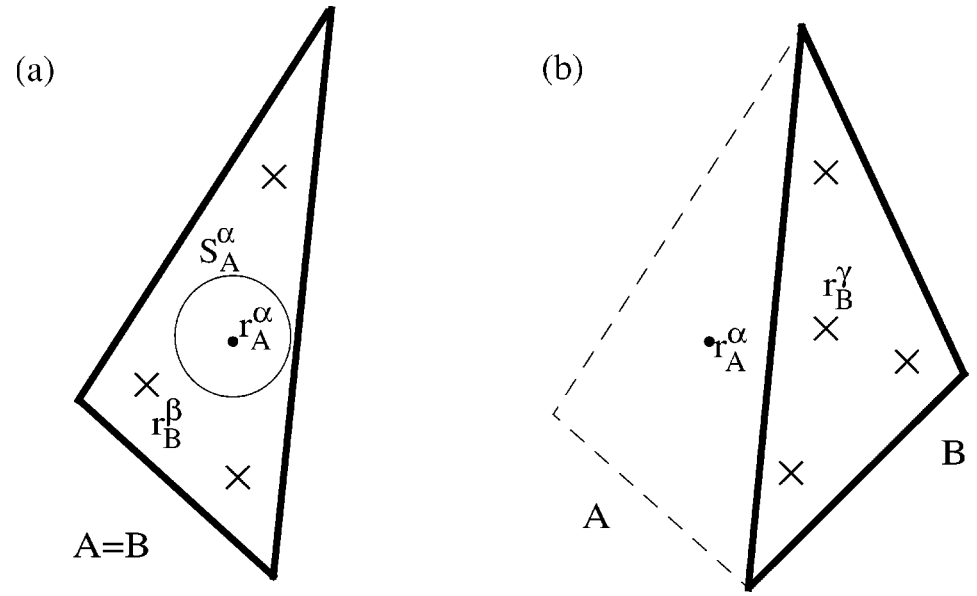

Fig. 2. (a) Gaussian integration is performed for $\mathbf{I}_{AA}^R$. Instead of the (undefined) value for $\mathbf{r}_A^\beta = \mathbf{r}_A^\alpha$ we take the integral inside a sphere of volume $w^\alpha J_A$. (b) The point $\mathbf{r}_B^\gamma$ for the regularization in (26)–(28) is the Gaussian point on B with the minimal distance to $\mathbf{r}_A^\alpha$.

respect to $|\mathbf{r}' - \mathbf{r}_A^\alpha|$. (Note that, for a regular function without singularity, Gaussian quadrature corresponds to retaining only the constant term and dropping the others.) For polynomial basis functions this leads to integrals that can be solved analytically.

To determine the integral $\mathbf{I}_{AA}^{\mathrm{S}}$, given by (18), one has two options: The first one is to take the Cauchy principal value by introducing an exclusion volume around the singularity, as done by Yaghian [15]. This approach is well suited for simple elements, like a sphere or a cube, where the integration on the element volume is easily performed [4]. For tetrahedral elements, however, the theory of generalized functions described by Gel'fand and Shirkov is more appropriate, since it reduces to integration on the element boundary [31].

Following this approach, we obtain after one partial integration for the mnth component of the tensor $\mathbf{I}_{AA}^{\mathrm{S}}$:

$$(I_{AA}^{\mathrm{S}})_{mn} = \phi^j(\boldsymbol{\xi}^\alpha)(-1)^{m-1}\int_{\partial\mathcal{V}_A} \partial_n g^{\mathrm{S}}(\mathbf{r}_A^\alpha, \mathbf{r}')\mathrm{d}r'_{p_1}\ldots\mathrm{d}r'_{p_n}, \quad p^i \neq m \tag{23}$$

with $\partial\mathcal{V}_A$ indicating the boundary of element A. As stressed by Lee *et al.*in a similar context [26], one can write this tensor as

$$\mathbf{I}_{AA}^{\mathrm{S}} = \phi^j(\boldsymbol{\xi}^\alpha)\,\frac{-1}{2(\mathrm{D}-1)\pi}\int_{\partial\mathcal{V}_A}\frac{\hat{\mathbf{N}}\mathbf{Q}}{Q^{\mathrm{D}}}\,\mathrm{d}\sigma. \tag{24}$$

Here $\hat{\mathbf{N}}$ is the unit outward normal vector on $\partial\mathcal{V}_A$, and $\mathbf{Q}$ is defined as $\mathbf{Q} = \mathbf{r}_A^\alpha - \mathbf{r}'$. This integral can be solved analytically.

Combining (21) and (24), we finally obtain the value of $\mathbf{I}_{AA}$ for identical elements

$$\mathbf{I}_{AA} = J_A \sum_{\beta=1,\,\beta\neq\alpha}^{\eta}\left\{w^\beta\left[\mathbf{G}(\mathbf{r}_A^\alpha, \mathbf{r}_A^\beta)\phi^j(\boldsymbol{\xi}^\beta) - \left(\frac{\nabla\nabla}{k_0^2}\,g^{\mathrm{S}}(\mathbf{r}_A^\alpha, \mathbf{r}_A^\beta)\right)\phi^j(\boldsymbol{\xi}^\alpha)\right]\right\}$$
$$+\int_{\mathcal{S}_A^\alpha}\mathrm{d}\mathbf{r}'\left[\mathbf{G}(\mathbf{r}_A^\alpha, \mathbf{r}')f_A^j(\mathbf{r}') - \left(\frac{\nabla\nabla}{k_0^2}\,g^{\mathrm{S}}(\mathbf{r}_A^\alpha, \mathbf{r}')\right)\phi^j(\boldsymbol{\xi}^\alpha)\right]$$
$$+\phi^j(\boldsymbol{\xi}^\alpha)\,\frac{-1}{2(\mathrm{D}-1)\pi}\int_{\partial\mathcal{V}_A}\frac{\hat{\mathbf{N}}\mathbf{Q}}{Q^{\mathrm{D}}}\,\mathrm{d}\sigma \tag{25}$$

where the integral over the sphere $\mathcal{S}_A^\alpha$ has to be solved as in (22).

3) Regularization of $\mathbf{I}_{AB}$ for Neighboring Elements: As discussed previously, even for different elements $A \neq B$, the evaluation of $\mathbf{I}_{AB}$ with Gaussian integration [(15)] can be inaccurate when $\mathbf{r}_A^\alpha$ is close to the element B [Fig. 2(b)]. It is, however, possible to apply a similar regularization scheme in that case.

As for identical elements, let us divide $\mathbf{I}_{\widetilde{AB}}$ into two parts (the tilde in $\widetilde{AB}$ indicates neighboring elements)

$$\mathbf{I}_{\widetilde{AB}} = \mathbf{I}_{\widetilde{AB}}^{\mathrm{R}} + \mathbf{I}_{\widetilde{AB}}^{\mathrm{S}} \tag{26}$$

with

$$\mathbf{I}_{\widetilde{AB}}^{\mathrm{R}} = \int_{\mathcal{V}_B}\mathrm{d}\mathbf{r}'\left[\mathbf{G}(\mathbf{r}_A^\alpha, \mathbf{r}')f_B^j(\mathbf{r}') - \left(\frac{\nabla\nabla}{k_0^2}\,g^{\mathrm{S}}(\mathbf{r}_A^\alpha, \mathbf{r}')\right)\phi^j(\boldsymbol{\xi}^\gamma)\right] \tag{27}$$

and

$$\mathbf{I}_{\widetilde{AB}}^{\mathrm{S}} = \phi^j(\boldsymbol{\xi}^\gamma)\int_{\mathcal{V}_B}\mathrm{d}\mathbf{r}'\,\frac{\nabla\nabla}{k_0^2}\,g^{\mathrm{S}}(\mathbf{r}_A^\alpha, \mathbf{r}'). \tag{28}$$

The Gaussian point $\boldsymbol{\xi}^\gamma$ in (27) is such that the corresponding global Gaussian point $\mathbf{r}_B^\gamma$ of (27) is the Gaussian point on tetrahedron B with the minimal distance to $\mathbf{r}_A^\alpha$ [Fig. 2(b)].

Applying Gaussian quadrature to $\mathbf{I}_{\widetilde{AB}}^{\mathrm{R}}$ and using (24) (which is also valid if $\mathbf{r}_A^\alpha$ is outside the integration region) we obtain

$$\mathbf{I}_{\widetilde{AB}} = \sum_{\beta=1}^{\eta}\left\{J_B w^\beta\left[\mathbf{G}(\mathbf{r}_A^\alpha, \mathbf{r}_B^\beta)\phi^j(\boldsymbol{\xi}^\beta) - \left(\frac{\nabla\nabla}{k_0^2}\,g^{\mathrm{S}}(\mathbf{r}_A^\alpha, \mathbf{r}_B^\beta)\right)\phi^j(\boldsymbol{\xi}^\gamma)\right]\right\}$$

$$- \phi^j(\boldsymbol{\xi}^\gamma) \frac{1}{2(\mathrm{D}-1)\pi} \int_{\partial \mathcal{V}_B} \frac{\hat{\mathbf{N}}\mathbf{Q}}{Q^{\mathrm{D}}} \mathrm{d}\sigma \tag{29}$$

which completes our general formalism.

III. Application of the Scheme for the 2-D-Case

The general scheme derived in the previous section will now be applied to the 2-D case, i.e., we assume a scatterer with an infinite symmetry axis in the z-direction. Furthermore, we assume that the wave vector $\mathbf{k}$ of the incident field is in the xy-plane (i.e., $k_z = 0, k_0 = k_\rho$). In that case the Green's tensor reads [4]

$$\mathbf{G}(\mathbf{r}, \mathbf{r}') = \left[\mathbf{1} + \frac{1}{k^2} \begin{pmatrix} \partial_x\partial_x & \partial_x\partial_y & 0 \\ \partial_x\partial_y & \partial_y\partial_y & 0 \\ 0 & 0 & 0 \end{pmatrix} \right] g(\mathbf{r}, \mathbf{r}') \tag{30}$$

with $g(\mathbf{r}, \mathbf{r}')$ now given by

$$g(\mathbf{r}, \mathbf{r}') = \frac{i}{4} \mathrm{H}_0^{(1)}(k_0 R) \tag{31}$$

with $\mathbf{r} = (x, y)$.

As implied by the form of the Green's tensor [(30)], we can distinguish two cases when the electrical field is polarized in z-direction [transverse magnetic (TM)] or when it is in the xy-plane [transverse electric (TE)].

We use triangular elements. The corresponding basis functions up to cubic order can be found in [11], [30], and [32], whereas appropriate Gaussian points up to order 10 can be found in [33]–[35]. Note that all the Gaussian points must be defined inside the element. The computation of the matrix elements b_A^{ij} and $\mathbf{e}_A^i$ is straightforward. We will only detail the procedure for $\mathbf{d}_{AB}^{ij}$, i.e., we give expressions for $\mathbf{I}_{AB}$ defined by (14) for identical and neighboring elements A and B.

A. TM Case

In the TM-case, the Green's tensor is given by the scalar Green's function itself, (31). Hence, no regularization is necessary and we only have to handle the weak singularity of the scalar Green's function as described in Section II-B.2. (Note that the formulas of the general description are still valid, but all the derivatives vanish since they are with respect to z in the TM-case.)

To determine I_{AA} (which now is a scalar), we first evaluate the analytical integral over $\mathcal{S}_A^\alpha$. Following (22) and expanding the last integrand in a Laurent series, we see that in the TM-case, for polynomial basis functions, this series does not have any singular or constant terms with respect to $|\mathbf{r}' - \mathbf{r}_A^\alpha|$. We can therefore omit it. Performing the other integral in (22), we finally obtain for I_{AA}

$$\begin{aligned} I_{AA} = {} & J_A \left(\sum_{\beta \neq \alpha}^{\eta} g(\mathbf{r}_A^\alpha, \mathbf{r}_A^\beta) w^\beta \phi^j(\boldsymbol{\xi}^\beta) \right) \\ & + \phi^j(\boldsymbol{\xi}^\alpha) \left(\frac{i\pi R_A^\alpha}{2k_0} H_1^{(1)}(k_0 R_A^\alpha) - \frac{1}{k_0^2} \right) \end{aligned} \tag{32}$$

with R_A^α the radius corresponding to $\mathcal{S}_A^\alpha$, namely

$$R_A^\alpha = \sqrt{\frac{w_\alpha J_A}{\pi}}. \tag{33}$$

Since a regularization scheme is not necessary for this polarization, neighboring elements can simply be treated with (15).

B. TE Case

In the TE-case, the Green's tensor is a 2×2 tensor, given by the xy-components of (30). To determine $\mathbf{I}_{AA}$ for identical elements, we first evaluate the analytical integral over $\mathcal{S}_A^\alpha$. Following (22) and expanding the last integrand in a Laurent series, it turns out that for polynomial basis functions all integrals over the relevant terms (i.e., the singular and constant terms with respect to $|\mathbf{r}' - \mathbf{r}_A^\alpha|$) vanish because of the integration over the polar angle φ. The other integral in (22) can easily be performed and (21) becomes

$$\begin{aligned} \mathbf{I}_{AA}^{\mathrm{R}} = {} & \sum_{\beta \neq \alpha}^{\eta} \Bigg[J_A w^\beta \Bigg(\mathbf{G}(\mathbf{r}_A^\alpha, \mathbf{r}_A^\beta) \phi^j(\boldsymbol{\xi}^\beta) \\ & - \phi^j(\boldsymbol{\xi}^\alpha) \frac{\nabla\nabla}{k_0^2} g^{\mathrm{S}}(\mathbf{r}_A^\alpha, \mathbf{r}_A^\beta) \Bigg) \Bigg] \\ & + \phi^j(\boldsymbol{\xi}^\alpha) \left(\frac{i\pi R_A^\alpha}{4k} H_1^{(1)}(kR_A^\alpha) - \frac{1}{2k^2} \right) \mathbf{1}. \end{aligned} \tag{34}$$

To determine the value of $\mathbf{I}_{AA}^{\mathrm{S}}$ given by (24), we parameterize the boundary $\partial \mathcal{V}_A$ of element A and determine its unit outward normal vectors. Defining $\mathbf{R}_A^4 \equiv \mathbf{R}_A^1$, the parameterization of the ith side of triangle A is given by

$$\mathbf{r'}^i{}_A(t) = (1-t)\mathbf{R}_A^i + t\mathbf{R}_A^{i+1}, \qquad t \epsilon [0, 1], i = 1, 2, 3 \tag{35}$$

and the unit outward normal vector $\mathbf{N}_A^i$ for this side is

$$\hat{\mathbf{N}}_A^i = \frac{1}{|\mathbf{R}_A^{i+1} - \mathbf{R}_A^i|} \begin{pmatrix} R_{A,2}^{i+1} - R_{A,2}^i \\ R_{A,1}^i - R_{A,1}^{i+1} \end{pmatrix}, \qquad i = 1, 2, 3. \tag{36}$$

Like this, (24) becomes

$$\begin{aligned} \mathbf{I}_{AA}^{\mathrm{S}} = {} & -\frac{1}{2\pi} \phi^j(\boldsymbol{\xi}^\alpha) \sum_{i=1}^{3} \\ & \cdot \left[\int_0^1 \mathrm{d}t \left(\frac{\mathbf{r}_A^\alpha - \mathbf{r'}^i{}_A(t)}{|\mathbf{r}_A^\alpha - \mathbf{r}_A^{i'}(t)|^2} \hat{\mathbf{N}}_A^i \right) \right] \\ = {} & \phi^j(\boldsymbol{\xi}^\alpha) \Bigg[\sum_{i=1}^{3} \Bigg(\frac{1}{2\pi} \hat{\mathbf{N}}_A^i \hat{\mathbf{N}}_A^i K_A^i \\ & - \frac{(\mathbf{R}_A^{i+1} - \mathbf{R}_A^i)}{4\pi |\mathbf{R}_A^{i+1} - \mathbf{R}_A^i|} \hat{\mathbf{N}}_A^i L_A^i \Bigg) \Bigg] \end{aligned} \tag{37}$$

where we introduced K_A^i and L_A^i given by

$$K_A^i = \log\left[(\mathbf{r}_A^\alpha - \mathbf{R}_A^i)^2\right] - \log\left[(\mathbf{r}_A^\alpha - \mathbf{R}_A^{i+1})^2\right] \tag{38}$$

$$\begin{aligned} L_A^i = {} & \arctan\left(\frac{\mathbf{N}_A^i \times (\mathbf{r}_A^\alpha - \mathbf{R}_A^i)}{\mathbf{N}_A^i \cdot (\mathbf{r}_A^\alpha - \mathbf{R}_A^i)} \right) \\ & - \arctan\left(\frac{\mathbf{N}_A^i \times (\mathbf{r}_A^\alpha - \mathbf{R}_A^{i+1})}{\mathbf{N}_A^i \cdot (\mathbf{r}_A^\alpha - \mathbf{R}_A^{i+1})} \right) \end{aligned} \tag{39}$$

where the 2-D vector product $\mathbf{a} \times \mathbf{b} \equiv a_1 b_2 - a_2 b_1$ is a scalar. The symmetry of the tensor $\mathbf{I}_{AA}^S$ is easily verified using the relation $\sum_{i=1}^3 K_A^{\alpha,\,i} = 0$.

With these results, $\mathbf{I}_{AA}$ reads

$$\mathbf{I}_{AA} = \mathbf{I}_{AA}^{\mathrm{R}} + \mathbf{I}_{AA}^{\mathrm{S}} \tag{40}$$

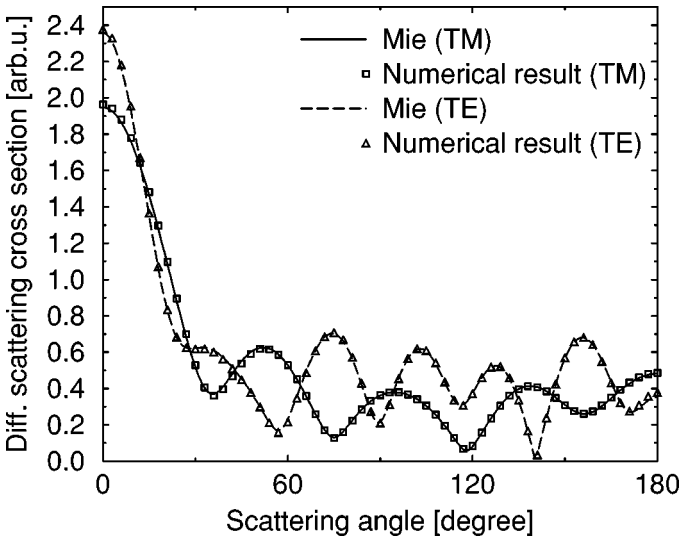

Fig. 3. Differential scattering cross section as a function of scattering angle for $\varepsilon = 4$ and size parameter $x = 10.43$, for both TM and TE polarization. The numerical results are compared to the reference solution obtained with Mie theory [30].

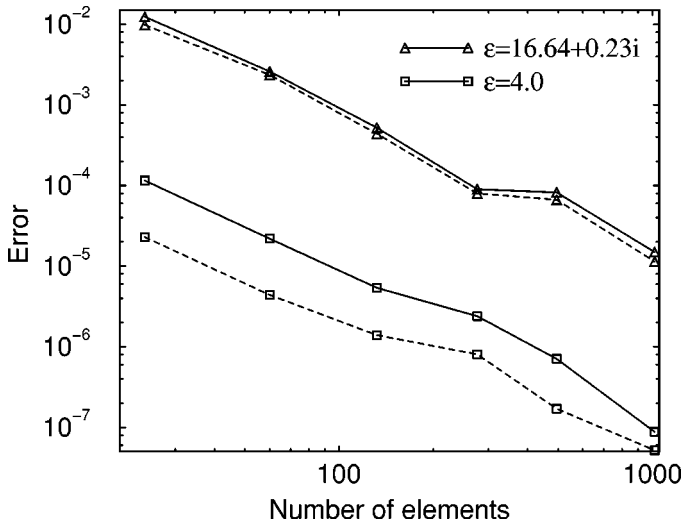

Fig. 4. Absolute error as a function of the number of elements for $\varepsilon = 4$ and $\varepsilon = 16.64 + 0.23i$ (Silicon) for both TE polarization (continuous line) and TM polarization (dashed line). ($\lambda = 546.1$ [nm] and cylinder diameter $d = 100$ [nm]).

with $\mathbf{I}^{\mathrm{R}}_{AA}$, respectively, $\mathbf{I}^{\mathrm{S}}_{AA}$, given by (34), respectively, (37).

For neighboring elements, we obtain

$$\mathbf{I}_{\widetilde{AB}} = \mathbf{I}^{\mathrm{R}}_{\widetilde{AB}} + \mathbf{I}^{\mathrm{S}}_{\widetilde{AB}} \tag{41}$$

with

$$\mathbf{I}^{\mathrm{R}}_{\widetilde{AB}} = \sum_{\beta=1}^{\eta} \Bigg[J_A w^{\beta} \Bigg(\phi^j(\boldsymbol{\xi}^{\beta}) \mathbf{G}(\mathbf{r}^{\alpha}_A, \mathbf{r}^{\beta}_B) - \phi^j(\boldsymbol{\xi}^{\gamma}) \frac{\nabla\nabla}{k_0^2} g^{\mathrm{S}}(\mathbf{r}^{\alpha}_A, \mathbf{r}^{\beta}_B) \Bigg) \Bigg] \tag{42}$$

and $\mathbf{I}^{\mathrm{S}}_{\widetilde{AB}}$ can be obtained from $\mathbf{I}^{\mathrm{S}}_{AA}$, (37)–(39), by the substitutions $\mathbf{r}^{i'}_A(t) \rightarrow \mathbf{r}^{i'}_B(t)$, $\phi^j(\boldsymbol{\xi}^{\alpha}) \rightarrow \phi^j(\boldsymbol{\xi}^{\gamma})$, $\mathbf{R}^i_A \rightarrow \mathbf{R}^i_B$, $\mathbf{N}^i_A \rightarrow \mathbf{N}^i_B$, where we want to keep in mind that the Gaussian point $\boldsymbol{\xi}^{\gamma}$ corresponds to the global Gaussian point $\mathbf{r}^{\gamma}_B$ with minimal distance to $\mathbf{r}^{\alpha}_A$ [Fig. 2(b)].

IV. 2-D Calculations

In this section, we present 2-D-calculations. To assess the accuracy of the numerical results we choose examples where an analytical solution exists. Throughout the examples we use constant basis functions and Gaussian points corresponding to order 7.

In the first example we compare the differential cross section for a cylinder ($\varepsilon = 4$, diameter d) for both TM and TE with the analytic Mie solution. The size parameter $x \equiv \pi\sqrt{\varepsilon} d/\lambda_0$ is 10.43.

As Fig. 3 implies, for a certain scattering angle we can define an error for the numerical result by taking the square of the difference between the numeric and analytic far-field amplitude, normalized to the square of the analytic far-field amplitude. Integration over the scattering angles gives us the absolute error of our result.

To show the convergence of our formalism, Fig. 4 gives this absolute error as a function of the number of elements used to discretize the geometry for both TM and TE polarization. The cylinder diameter is 100 [nm] and the wavelength 546 [nm]. We show the result for $\varepsilon = 4$ and $\varepsilon = 16.65 + 0.23i$, the latter corresponding to silicon at that wavelength [1]. We see that even with few elements, the formalism gives very accurate results including for bodies with a high permittivity.

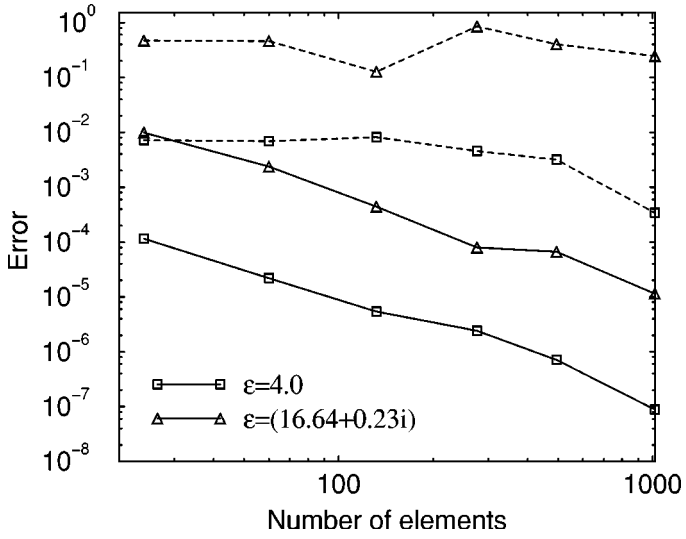

Fig. 5. Absolute error as a function of the number of elements for TE polarization with (continuous line) and without (dashed line) the regularization for neighboring elements. (Same parameters as in Fig. 4.)

To demonstrate the importance of the regularization for neighboring elements presented in Section II-B.3, we compare in Fig. 5 the error of the numerical result with and without this regularization for TE polarization. We use the same parameters as in Fig. 4. These results emphasize the importance of the regularization for neighboring elements.

Dispersive materials like silver are known to exhibit a resonant behavior at particular optical wavelengths (plasmon– polariton) [36]. Many numerical methods are known to be inac-

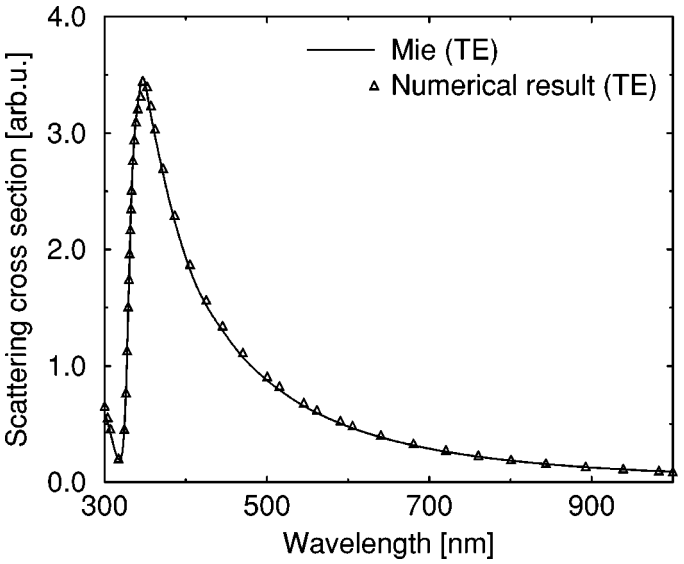

Fig. 6. Scattering cross section as a function of the wavelength for a silver cylinder (diameter $d = 100$ [nm]), for TE polarization. The plasmon resonance at 347 [nm] is very well reproduced with our approach.

curate at the resonance. The scattering cross section of a silver cylinder with diameter $d = 100$ [nm] is represented in Fig. 6 as a function of the wavelength of the incident TE field (TM does not exhibit resonant behavior), 132 triangles were used. The resonance is very well reproduced by the present method.

In our numerical calculations, it turns out that higher-order basis functions like linear or quadratic basis functions provide even better results in the TM-case for the same number of elements. This is also the case for TE polarization. However, for a very small ratio of the element length to the wavelength, constant basis functions give better results for TE polarization. This surprising issue may be understood in the following manner: For very small elements (compared to the wavelength) a constant basis function can approximate the field over the element very well and therefore the natural advantage of high-order basis functions decreases. Furthermore, for higher-order basis functions, the size and the condition of the system of equations increase rapidly. Finally, for small elements, the Gaussian points lie very close to each other and the regularization procedure becomes extremely important. This regularization procedure is most accurate for constant basis functions since then $f_A^j(\mathbf{r}') = \phi^j(\boldsymbol{\xi}^\alpha)$ [(17)].

V. Conclusion

We applied the method of moment to the VIE using 3-D and 2-D elements. We presented a regularization scheme to handle the strong singularity of the Green's tensor. This regularization scheme was further developed to take into account neighboring elements, which strongly enhanced the accuracy and the convergence of the method. The formalism was given in a general way that can be easily implemented for 3-D systems. We demonstrated that our approach is well suited for scattering calculations in high-permittivity materials. Furthermore, we were able to accurately reproduce the plasmon resonances in small metallic particles.

Acknowledgment

The authors would like to thank D. Fredkin, S. Schultz, and D. Smith for stimulating discussions.

References

[1] Landolt-Börnstein, *Numerical Data and Functional Relationships in Science and Technology*. Berlin: Springer-Verlag, 1982, vol. 17a, Semiconductors.

[2] P. Gay-Balmaz and J. R. Morsig, "3D planar radiating structures in stratified media," *Int. J. Microwave Millimeter Wave CAE*, vol. 3, pp. 330–343, 1997.

[3] E. M. Purcell and C. R. Pennypacker, "Scattering and absorption of light by nonspherical dielectric grains," *Astrophys. J.*, vol. 186, pp. 705–714, 1973.

[4] O. J. F. Martin and N. B. Piller, "Electromagnetic scattering in polarizable backgrounds," *Phys. Rev. E*, vol. 58, no. 3, pp. 3909–3915, 1998.

[5] M. F. Iskander, H. Y. Chen, and J. E. Penner, "Optical scattering and absorption by branched chains of aerosols," *Appl. Opt.*, vol. 28, no. 15, pp. 3083–3091, 1989.

[6] C. E. Dungey and C. F. Bohren, "Light scattering by nonspherical particles: A refinement to the coupled-dipole method," *J. Opt. Soc. Amer. A*, vol. 8, no. 1, pp. 81–87, 1991.

[7] N. B. Piller and O. J. F. Martin, "Increasing the performances of the coupled-dipole approximation: A spectral approach," *IEEE Trans. Antennas Propagat.*, vol. 46, pp. 1126–1137, Aug. 1998.

[8] B. T. Draine and P. J. Flatau, "Discrete-dipole approximation for scattering calculations," *J. Opt. Soc. Amer. A*, vol. 11, no. 4, pp. 1491–1499, 1994.

[9] J. H. Richmond, "A wire grid model for scattering by conducting bodies," *IEEE Trans. Antennas Propagat.*, vol. 14, pp. 782–786, June 1966.

[10] D. H. Schaubert, D. R. Wilton, and A. W. Glisson, "A tetrahedral modeling method for electromagnetic scattering by arbitrarily shaped inhomogeneous dielectric bodies," *IEEE Trans. Antennas Propagat.*, vol. AP-32, pp. 77–85, 1984.

[11] P. P. Silvester and R. L. Ferrari, *Finite Elements for Electrical Engineers*, 2nd ed. Cambridge, U.K.: Cambridge Univ. Press, 1990.

[12] R. D. Graglia, "The use of parametric elements in the moment method solution of static and dynamic volume integral equations," *IEEE Trans. Antennas Propagat.*, vol. 36, pp. 636–646, May 1988.

[13] J. L. Volakis, A. Chatterjee, and L. C. Kempel, "Review of the finite-element method for three-dimensional electromagnetic scattering," *J. Opt. Soc. Amer. A*, vol. 11, no. 4, pp. 1422–1433, 1994.

[14] D. R. Wilton, "Review of current status and trends in the use of integral equations in computational electromagnetics," *Electromagnetics*, vol. 12, pp. 287–341, 1992.

[15] A. D. Yaghjian, "Electric dyadic Green's functions in the source region," *Proc. IEEE*, vol. 68, pp. 248–263, 1980.

[16] C.-T. Tai, *Dyadic Green Function in Electromagnetic Theory*. New York: IEEE Press, 1994.

[17] A. P. Papagiannakis, "Application of a point-matching mom reduced scheme to scattering from finite cylinders," *IEEE Trans. Microwave Theory Tech.*, vol. 45, pp. 1545–1553, Sept. 1997.

[18] C.-T. Tsai, H. Massoudi, C. H. Durney, and M. F. Iskander, "A procedure for calculating fields inside arbitrarily shaped, inhomogeneous dielectric bodies using linear basis functions with the moment method," *IEEE Trans. Microwave Theory Tech.*, vol. 34, pp. 1131–1138, Nov. 1986.

[19] A. P. M. Zwamborn and P. M. van den Berg, "The three-dimensional weak form of the conjugate gradient FFT method for solving scattering problems," *IEEE Trans. Microwave Theory Tech.*, vol. 40, pp. 1757–1766, Sept. 1992.

[20] M. F. Catedra, E. Gago, and L. Nuño, "A numerical scheme to obtain the RCS of three-dimensional bodies of resonant size using the conjugate gradient method and the fast fourier transform," *IEEE Trans. Antennas Propagat.*, vol. 37, pp. 528–537, May 1989.

[21] H. Gan and W. C. Chew, "A discrete BCG-FFT algorithm for solving 3-D inhomogeneous scatterer problems," *J. Electromagn. Waves Applicat.*, vol. 9, no. 10, 1995.

[22] Y. A. Eremin and V. I. Ivakhnenko, "Modeling of light scattering by nonspherical inhomogeneous particles," *J. Quant. Spectrosc. Radiat. Transfer*, vol. 60, no. 3, pp. 1–8, 1998.

[23] T. K. Sarkar, S. M. Rao, and A. R. Djordjevic, "Electromagnetic scattering and radiation from finite microstrip structures," *IEEE Trans. Microwave Theory Tech.*, vol. 38, pp. 1568–1575, Nov. 1990.

[24] D. A. Vechinski, S. M. Rao, and T. K. Sarkar, "Transient scattering from three-dimensional arbitrarily shaped dielectric bodies," *J. Opt. Soc. Amer. A*, vol. 11, no. 4, pp. 1458–1469, 1994.
[25] L. Mendes and E. Arvas, "TE-scattering from dense homogeneous infinite dielectric cylinders of arbitrary cross-section," *IEEE Trans. Magn.*, vol. 27, pp. 4295–4298, May 1991.
[26] S.-W. Lee, J. B. Boersma, C.-L. Law, and G. A. Deschamps, "Singularity in Green's function and its numerical evaluation," *IEEE Trans. Antennas Propagat.*, vol. 28, pp. 311–317, Mar. 1980.
[27] D. R. Wilton and C. M. Butler, "Effective methods for solving integral and integro-differential equations," *Electromagnetics*, vol. 1, no. 3, pp. 289–308, 1981.
[28] S. A. Jenkins and J. R. Bowler, "Numerical evaluation of singular matrix elements in three dimensions," *IEEE Trans. Magn.*, vol. 27, pp. 4438–4444, June 1991.
[29] J. Rejeb, T. Sarkar, and E. Arvas, "Extension of the MoM Laplacian solution to the general Helmholtz equation," *IEEE Trans. Microwave Theory Tech.*, vol. 43, pp. 2579–2584, Nov. 1995.
[30] O. C. Zienkiewicz and R. L. Taylor, *The Finite Element Method*. London: McGraw-Hill, 1967.
[31] I. M. Gel'fand and G. E. Shirkov, *Generalized Functions*. New York: Academic, 1964.
[32] K. W. Morton, "Basic course in finite element methods," *Comput. Phys. Rep.*, vol. 6, pp. 1–72, 1987.
[33] G. R. Cowper, "Gaussian quadrature formulas for triangles," *Int. J. Numer. Methods Eng.*, vol. 7, no. 3, pp. 405–408, 1973.
[34] P. Hillion, "Numerical integration on a triangle," *Int. J. Numer. Methods Eng.*, vol. 11, pp. 797–815, 1977.
[35] K. S. Sunder and R. A. Cookson, "Integration points for triangles and tetrahedrons obtained from the Gaussian quadrature points for a line," *Comput. Struct.*, vol. 21, no. 5, pp. 881–885, 1985.
[36] C. F. Bohren and D. R. Huffman, *Absorption and Scattering of Light by Small Particles*. New York: Wiley, 1983.

Jörg P. Kottmann received the Dipl.-Phys. degree from Freie Universität Berlin, Germany, in 1997 and is currently working toward the Ph.D. degree at the Swiss Federal Institute of Technology (ETH) Zurich, Switzerland.

After working with Daimler-Chrysler-Aerospace Dornier GmbH, he joined the Electromagnetic Fields and Microwave Electronics Laboratory of the Swiss Federal Institute of Technology (ETH) Zurich, Switzerland, in June 1998. His research interests include the development of computational techniques for electromagnetic scattering and the investigation of the plasmon resonances in small metal structures of nonregular shape.

Olivier J. F. Martin received the undergraduate and Ph.D. degrees in physics in 1989 and 1994, respectively, from the Swiss Federal Institute of Technology, Lausanne (EPFL), Switzerland.

In 1989, he joined IBM Zurich Research Laboratory, where he investigated the thermal and optical properties of semiconductor laser diodes. Since 1994, he has been Research Staff Member at the Swiss Federal Institute of Technology Zurich (ETHZ). Currently, his research interests are focused on the analysis of the interaction of electromagnetic fields with small dimension systems, with an emphasis on local probe microscopes (scanning tunneling microscope, scanning near-field optical microscope), photonic bandgap structures and integrated optics. In 1997, he received a special tenure fellowship from the Swiss National Science Foundation and since 1998, he has been Lecturer at ETHZ.

Dr. Martin was awarded the Latsis prize for contributions in the domain of local probe techniques and photonic bandgap structures in 1999.